Progress in Additive Manufacturing (2024) 9:2061–2071
https://doi.org/10.1007/s40964-023-00562-0

FULL RESEARCH ARTICLE

Characterizing photopolymer resins for high-temperature vat photopolymerization

Viswanath Meenakshisundaram[1,2] · Keyton Feller[2] · Nicholas Chartrain[2,3] · Timothy Long[4] · Christopher Williams[1,2]

Received: 11 September 2023 / Accepted: 25 December 2023 / Published online: 20 February 2024

Abstract

The availability of engineering polymers for vat photopolymerization (VP) additive manufacturing is limited. This limitation primarily stems from the inability of standard VP systems to recoat high-viscosity resins (> 3 Pa s). High-temperature vat photopolymerization is a new process-based VP platform that enables processing of viscous photopolymer resins (viscosity > 3 Pa s). Research in this area has been focused on demonstrating expanded access to new polymer families, and studying the effect of printing temperature on mechanical and esthetic performance of printed parts. However, methods to determine the printing temperature that prevents the occurrence of thermally induced polymerization (i.e., thermal stability) in the resin have not been established. In this work, the authors have applied characterization techniques such as thermogravimetric analysis, Rheology and differential scanning calorimetry to determine the printing temperature for processing viscous photopolymer resins. As a case study, the developed characterization techniques are applied to: (1) photopolymer that is solid at room temperature, (2) polymer with viscosity of 21 Pa s at room temperature, and the temperature at which the resins can be printed without triggering thermally induced polymerization is successfully determined. The results of this work will act as a materials' characterization and process parameter development guide for high-temperature VP systems, thus enabling expansion of VP materials catalogue to engineering materials that were previously unprocessable.

Keywords Hot lithography · Vat photopolymerization · Stereolithography · Viscous photopolymers

1 Introduction

Vat photopolymerization (VP) is a polymer additive manufacturing (AM) process wherein the resin surface is selectively exposed to ultra-violet (UV) light to convert irradiated regions from a liquid to solid state [1, 2]. VP is commonly used to prototype complex geometries because of its ability to manufacture parts with attributes such as: high-feature resolution, superior surface finish, and high-manufacturing speed [3–5]. While VP systems have been able to meet these manufacturing metrics for prototypes by using low viscosity resins (< 3 Pa s) [6], meeting the demand for manufacturing end use products with complex geometries and superior material properties has necessitated the migration towards the development and use of engineering photopolymers [1, 2]. Among the different strategies available for vat photopolymerization of engineering photopolymers, the route of using high-viscosity resins to access engineering polymers has become popular because it offers the following advantages:

✉ Christopher Williams
cbwill@vt.edu

Viswanath Meenakshisundaram
vmeenak@vt.edu

Keyton Feller
kfeller@vt.edu

Nicholas Chartrain
nickchar@vt.edu

Timothy Long
Timothy.E.Long@asu.edu

[1] Department of Mechanical Engineering, Virginia Tech, Blacksburg, VA 24061, USA

[2] Macromolecules Innovation Institute, Virginia Tech, Blacksburg, VA 24061, USA

[3] Department of Material Science and Engineering, Virginia Tech, Blacksburg, VA 24061, USA

[4] School of Molecular Sciences, Arizona State University, Tempe, AZ 85281, USA

1. *Improvement in thermo-mechanical performance* High viscosity photopolymers often use blends of high molecular weight backbones with oligomeric moieties. These inclusions can positively affect the mechanical performance in areas such as toughness, elongation at break, and modulus. This strategy offers a path to use photopolymers for engineering applications [7]
2. *Predictable control of geometry* Reduction in use of viscosity modifiers such as volatile monomers, solvents (reactive and unreactive) [8, 9] reduces evaporative losses during post-processing and lowers post-process complexity. Reduced shrinkage allows the use of simple design compensation techniques such as global scaling, uniform Z-compensation to predictably manufacture complex parts with features across comparable size scales.

Traditional VP systems find it challenging to handle high-viscosity polymers. One of the sources for this limitation is the fluid dynamics occurring during the recoating step. In passive recoating systems where resin is allowed to settle under self-weight (Top Down or free-surface VP systems) or allowed to flow due to pressure head (Bottom up or constrained surface VP system), the rate of flow, settling time, and distance of resin travel are dependent on the viscosity of the resin [10]. Increase in resin viscosity increases settling time, lowers recoat quality and manufacturing throughput. While addition of active elements such as recoating blades, recirculation units, or tilting elements help mitigate the issues, the complex fluid dynamic interactions introduced by the inclusion of such elements (i.e., drag force on the printed parts, pressure differentials created by hollow areas) still make them inefficient while processing viscous resins [10–14]. Another challenge with viscous photopolymers is poor/slow reaction kinetics. Highly viscous photopolymer systems offer low mobility to reactive species which leads to poor conversion or insufficient curing that results in green parts that are incapable of supporting self-weight or shape [15]

Hot lithography, or high-temperature VP, is a VP platform wherein the photopolymer resin is heated to elevated temperatures to lower the resin viscosity within the processible limits of the VP apparatus. The use of high-temperature VP apparatus for manufacturing complex, high-resolution features with highly viscous resins has already been demonstrated [16–18]. Majority of the high-temperature VP research has been focused on understanding the effect of elevated printing temperature on the % conversion and thermo-mechanical properties of the printed parts [19]. While prior research has been successful in demonstrating the ability of high-temperature VP systems to handle viscous photopolymers, the tools and techniques to help VP users study, characterize and develop printing parameters for high temperature VP systems remain unexplored. This exploration is even more pertinent given that it is known that acrylate systems have a tendency to undergo thermally induced polymerization at high-temperatures [20].

To this end, the primary objective of this work is to present a set of characterization techniques that can be used to determine the safe printing temperature for high-temperature VP systems. Specifically, this work details the application of the proposed characterization techniques to two case unique high-viscosity photopolymer systems. The methods to analyze and interpret the characterization results for process parameter selection are presented. The proposed methods are then validated using the predicted printing parameters for actual part fabrication using a custom high-temperature VP setup. The results of this work will help provide insight into the thermal stability of photopolymer resins and enable successful printing of previously inaccessible polymers.

2 Materials and methods

Two material systems exhibiting the following characteristics were selected as case studies: (1) high viscosity at room temperature (urethane acrylate), and (2) solid at room temperature (Bisphenol A dimethacrylate) (Sect. 2.1). Characterization techniques developed to determine safe processing temperatures, i.e., process these materials without initiating thermally induced polymerization are outlined in Sect. 2.2. The design and construction of the high-temperature VP apparatus is outlined in Supplementary Information (SI) Section S1. Methods for specimen fabrication and post-processing are detailed in Sect. 2.3.

2.1 Materials

2.1.1 Solid photopolymer resin (BPADMA)

Bisphenol-A-dimethacrylate (BPADMA), a solid at room temperatures, was procured from Sigma Aldrich (SKU: 156329). Diphenyl (2,4,6-trimethylbenzoyl) phosphine oxide (TPO), a photoinitiator, was procured from TCI chemicals (D3358). BPADMA was heated to 100 °C (melting point: 72–74 °C) and brought to liquid state. TPO (melting point: 88–92 °C) was then added to the liquid BPADMA in the ratio of 1:100 by weight (TPO:BPADMA). The mixture was cooled to room temperature before printing.

2.1.2 High-viscosity photopolymer resin (EBECRYL-242)

A premixed resin containing aliphatic urethane acrylate oligomer and isobornyl acrylate (IBOA) (30 wt% IBOA)

was procured from Allnex (EBECRYL-242). 1 wt% of TPO (with respect to the resin) was dissolved in 10 ml. of chloroform and mixed into the resin. The mixture was heated to 60 ° C and stirred to remove the chloroform. The mixture was cooled to room temperature before printing.

2.2 Resin characterization techniques

2.2.1 Thermogravimetric analysis (TGA)

To determine the thermal degradation temperature (T_d), BPADMA and EBECRYL-242 resins were subjected to thermogravimetric analysis. Specimens were placed in platinum pans in TA instruments Q50 TGA instrument. Samples were heated in air from 25 to 600 °C at a constant heating rate of 10 °C/min.

2.2.2 Variable-temperature rheology

Thermal polymerization temperature (T_p) is the temperature at which the onset of thermally induced polymerization is observed. At T_p, the photopolymer resin is expected to exhibit an increase in viscosity due to thermally induced polymerization. To determine T_p, first the photopolymer resins were loaded onto the parallel plate geometry (40 mm diameter) in a TA Discovery HR2 rheometer. BPADMA resin was heated to an initial temperature of 90 °C, for melting, whereas the EBECRYL-242 resin was loaded at room temperature. The samples were then subjected to an oscillatory shear rate of 1 Hz. A temperature ramp of 2 °C/minute was applied until a rapid increase in viscosity ($\Delta\eta >$ order of magnitude) was observed. Following this, the temperature (T_p) was recorded and the experiment was terminated to prevent the parallel plates from adhering together.

2.2.3 Differential scanning calorimetry (DSC) of BPADMA

DSC was used to determine the maximum printing time (t_{max}) before which thermally induced polymerization was observed at elevated operating temperatures. The occurrence of an exotherm was used as an indicator of thermally induced polymerization. Based on the T_p and T_d determined from rheology and TGA, respectively, isothermal DSC was conducted for BPADMA resin between 90 and 115 °C at 5 °C increments. DSC was performed on the EBECRYL-242 resin at 75 °C because heating it beyond 75 °C resulted in monomer volatilization. The duration of the isotherms were selected based on typical printing time of 60 min to ensure thermal polymerization would not occur in the vat during part fabrication. The isothermal DSC experiments were performed on a TA Q1000 DSC instrument with the resins in T-0 aluminum pans. Samples were subjected to 10 °C/min ramp to the isotherm temperatures held for 60 min and then 10 °C/min ramp to the next isotherm temperature. The experiment was terminated upon onset of thermally induced polymerization or degradation.

2.3 Specimen fabrication

2.3.1 Prototype of the high-temperature VP apparatus

The prototype of the constructed high-temperature VP apparatus is shown in Fig. 1. The body of the prototype was constructed from aluminum extrusions. The vat was machined from aluminum for high-temperature operation and resistance to solvents in photopolymer resins. A rotary recoating system, driven by a single high torque stepper motor, was incorporated into the machine. The recoating blade and the build platform were constructed using stainless steel sheets for high-temperature operation. The build platform was attached to a linear stage (V-slot NEMA 23-OpenBuilds). The linear stage did not exhibit signs of backlash or degradation in performance

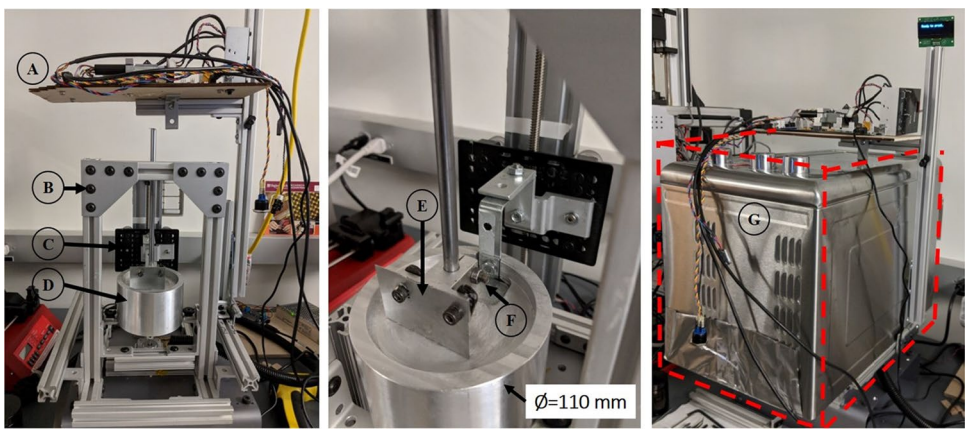

Fig. 1 Prototype of the high-temperature vat photopolymerization apparatus. **A** Optics and electronics, **B** aluminum frame, **C** Z-stage, **E** stainless steel recoating blade, **F** stainless steel recoating platform, **G** convection heating chamber, red dashed line heated zone

when heated to 200 °C. The stepper motors (NEMA 23), used to drive the linear stage and the recoating mechanism, were placed outside the heating zone. Since the current recoating and Z-stage designs eliminate the need for belts, pulleys and lubricants, the system is expected to exhibit high dimensional accuracy and reliability during high-temperature operation. The light engine, comprising of a 65 mw 405 nm UV laser, optical train and control circuits were extracted from a commercial VP system (Formlabs 1+, Formlabs-Boston, MA). Care was taken to ensure that the optical travel length remained unchanged in the new setup. A custom Arduino based controller was used to synchronize the recoating system and the build platform with the toolpath generated by the commercial VP system.

The heating chamber was constructed by modifying a commercial convection heating unit with active temperature monitoring system. The heating system was seated over the vat, resin, build stage and recoating mechanism. Experimental verification of this lumped capacitance setup revealed that the designed system was capable of maintaining uniform temperature within the resin (Section S1—Supplementary Information (SI), Figure S1a).

2.3.2 Working curve generation

Resin characterization, Sects. 2.2 and 3.1, enabled determination of the printing temperature T_{print}: 90 °C for BPADMA and 75 °C for the EBECRYL-242 resins. Resins were transferred to the vat and heated to T_{print}. Upon reaching steady state temperature, the resins were maintained at T_{print} for 15 min. The build platform was removed from the machine and five square profiles (5 × 5 mm) were scanned on the free-resin surface. Curing the profiles without a build stage allowed unrestricted growth of cure profile, thus providing a realistic estimate of the cure depth. Cured films, floating on the resin surface, were removed from the vat and subjected to post-processing (Sect. 2.3.4). A micrometer was used to measure the thickness of the cured films (measurement location: center, 5 samples/dosing energy).

The following exposure settings were selected for the BPADMA resin: Laser power of 25 mW, hatch spacing of 0.09 mm, and scan velocities of 1350, 1200, 1050, 900, and 750 mm/s. The following exposure settings were selected for the EBECRYL-242 resin: Laser power of 62 mW, hatch spacing of 0.09 mm, and scan velocities of 1550, 1400, 1300, 1200, and 1000 mm/s. The depth of penetration (D_p) and critical energy (E_c) for BPADMA and EBECRYL-242 resins were determined by generating working curves using the measured film thickness and corresponding UV exposures [21] (SI-Figure SI 5).

2.3.3 Part fabrication

A hexagonal lattice and rook were selected to test the ability to manufacture specimens with complex geometry and high-feature resolution. Formlabs Preform software (Version 2.3.3) was used to generate the laser toolpath for the test specimens at a layer thickness of 120 µm. Liquefied resin was then transferred into the vat. The heating chamber was placed over the vat and the printing temperature (T_{print}) was set based on the resin. Following the fabrication of each layer, the build platform was lowered into the vat by the layer thickness, and a fresh layer of resin was delivered to the build platform by the recoating mechanism. Following the initial adhesion passes, model layers were fabricated with one pass of the laser. The print parameters used for fabrication of the BPADMA and EBECRYL-242 resins are listed in Table 1.

2.3.4 Post-processing

After completion of part fabrication, parts printed with BPADMA were extracted from the build platform and dipped in olive oil (Filippo Berio Extra Virgin Olive Oil) maintained at the same temperature as T_{print} and then slowly cooled to room temperature. Once the oil reached room temperature, the annealed parts were removed from the oil and wiped dry with Kimwipes. Parts were rinsed in chloroform and compressed air was used to dry the parts completely. Following the drying step, the specimens were then post-cured for 60 min in a Melodysusie UV chamber, at room temperature, to photocure any uncured monomer in the printed part.

Parts printed with EBECRYL-242 were extracted from the build platform and immersed in a vial containing Ethanol. After 15 min of agitation, parts were removed and rinsed with Ethanol to remove any trace resin residue. Rinsed parts were dried with compressed air and tapped dry with Kimwipes. The specimens were then post-cured for 60 min in a

Table 1 Printing parameters used for specimen fabrication

Printing parameter	BPADMA	EBECRYL-242
Printing temperature (°C)	90	75
Depth of penetration (D_p) (µm)	480	310
Critical Energy (E_c) (mJ)	0.05	0.33
Layer thickness (µm)	120	120
Scan speed (V_s) (mm/s)	1550	1400
Laser power (P) (mW)	25	62
No. of laser passes for adhesion layers	10	3
No. of laser passes for model layers (N)	1	1
Hatch spacing (h) (mm)	0.09	0.09

Melodysusie UV chamber, at room temperature, to photocure any uncured oligomer in the printed part.

2.3.5 Tensile testing

Micro-tensile specimens based on ASTM D638 were fabricated and post-processed using the parameters listed in Sects. 2.3.3 and 2.3.4, respectively. Parts were subjected to uniaxial tensile testing using Instron 5984. Specimens were subjected to an extension rate of 5 mm/s and the loads were captured using a 100 kN load cell. The elongation and ultimate tensile strength calculated by the bluehill software were directly reported in the manuscript.

3 Results and discussion

3.1 Resin characterization for high-temperature printing

Accurate determination of the temperature at which thermally induced polymerization occurs (T_p) is critical for successful part fabrication with the designed high-temperature VP apparatus. To this end, the resins were subjected to characterization techniques outlined in Sect. 2.2.

3.1.1 Probing the onset of thermal degradation

For successful printing of EBECRYL-242 and BPADMA resin, it is imperative that the resins do not undergo thermal degradation or volatilization at elevated operating temperatures. A weight loss of 1% was considered to be an indicator for onset of degradation or volatilization. TGA of BPADMA resin, shown in Fig. 2, reveals that the resin is stable up to temperatures of 200 °C, thus indicating it can be heated to high temperatures without undergoing degradation.

EBECRYL-242 resin, however, shows 1% weight loss at 75 °C, as observed in Fig. 2. Heating beyond 75 °C resulted in rapid weight loss. This weight loss could be attributed to (1) volatilization of residual chloroform that was used to dissolve the photoinitiator, (2) volatilization of the reactive diluent IBOA and other trace additives, and (3) volatilization of aliphatic urethane acrylate oligomers. To investigate this hypothesis, a small batch of EBECRYL-242 without photoinitiator and chloroform was subjected to isothermal TGA at 100 °C. A weight loss of 25 %, which is comparable to the weight of IBOA (30 wt%) added to the resin, was observed (SI, Figure SI 3(A)). Given that the boiling point of IBOA is 120 °C, it is likely that the weight loss observed between 75 and 100 °C is primarily due to the volatilization of IBOA. The subsequent weight loss observed beyond 100 °C is likely from volatilization of trace amounts of IBOA and the urethane oligomers.

To confirm the observed mass loss is primarily due evaporation and not due to degradation, a fully photocured specimen of EBECRYL-242 was subjected to TGA (SI, Figure SI 3(B)). A mass loss of 5 wt% was observed until 180 °C, beyond which the mass loss stabilized until onset of degradation around 280 °C [22]. Given the slow and gradual nature of mass loss under 180 °C, it can be concluded that the mass loss observed between 75 and 180 °C is primarily due to volatilization of the residual uncured oligomer and reactive diluent and not due to degradation.

In the context of EBECRYL-242, volatilization of resin constituents at elevated temperatures may lead to change in resin composition during printing. This may lead to change in cured network composition and result in non-isotropic

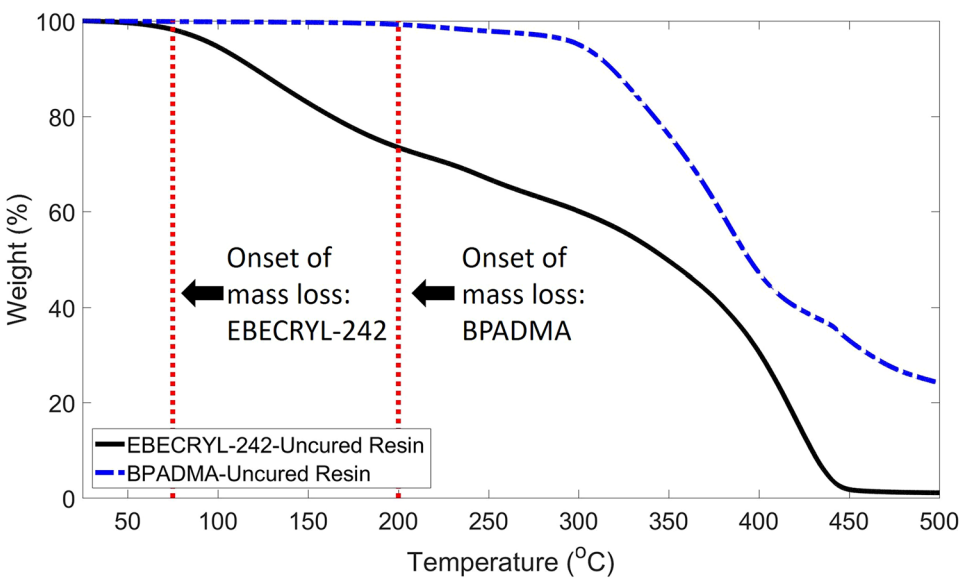

Fig. 2 TGA of EBECRYL-242 resin exhibits weight loss due to IBOA volatilization at 75 °C. TGA of BPADMA indicates it can be processed without chemical degradation or volatilization up to operating temperatures of 200 °C

mechanical properties. Therefore, the maximum printing temperatures for EBECRYL-242 were selected to be 75 °C.

It must be highlighted that more advanced characterization techniques such as TGA-MS can accurately determine the composition of the volatile matter. However, in this instance, selection of a temperature that prevented the occurrence of volatilization was assumed to be more significant for successful part fabrication. Analysis of the volatiles will be conducted in future publications.

3.1.2 Exploring susceptibility to thermally induced polymerization

As resins are heated to elevated temperatures, the probability of thermally initiated polymerization reactions increases. At the onset of polymerization, the formation of crosslinked polymer chains will increase the resin viscosity. Since the rheometer is capable of accurately capturing small changes in resin viscosity, subjecting the resins to variable-temperature rheology will help in capturing these polymerization events. The temperature at which thermally induced polymerization occurs (T_p) can be captured by identifying the temperature at which a sharp, continuous increase in viscosity is observed.

Starting as a solid at room temperature, BPADMA resin exhibited reduction in viscosity when it was heated from 90 to 118 °C. It must be noted that the sharp transitions observed between 90 and 118 °C are artifacts arising in the instrument due to very low viscosity values (10^{-2} Pa s). At 118 °C, the resin exhibited a sharp increase in viscosity ($\Delta\eta > 10^3$), thus indicating the occurrence of thermally induced polymerization, as shown in Fig. 3. DSC was performed to confirm the occurrence of polymerization. DSC of BPADMA at 110 °C reveals that the shape of the exotherm peak is skewed right (Fig. 4), thus confirming the occurrence of free radical polymerization [23].

Since heating EBECRYL-242 above 75 °C resulted in volatilization, the rheology experiment was conducted only up to 75 °C. The absence of an upward trend in the viscosity in Fig. 3 reveals that EBECRYL-242 resin does not undergo thermally induced polymerization at temperatures below 75 °C. It must be noted that heating the resin beyond 100 °C resulted in the generation of white fumes from the instrument. This observation, along with the weight loss observed during TGA (Fig. 2, SI-Figure SI 3(A)), substantiates the hypothesis that volatilization occurs before the resin undergoes thermally induced polymerization.

3.1.3 Exploring effect of processing time on thermal stability

While the variable-temperature rheology experiment helps in determining the onset of thermally induced polymerization (T_p), T_p only reflects the polymerization temperature at high heating rates, i.e., it does not capture the effect of heating the polymer for prolonged periods of time when $T_{print} < T_p$. The dependence of thermal stability over time was probed using a DSC instrument at various isotherms, listed in Sect. 2.2.3. Since a polymerization event is exothermic, the time at which a polymerization event (i.e., the onset of an exotherm) occurs can be easily captured in a DSC instrument by holding the resin at elevated temperatures ($T < T_p$) for extended periods of time. The isotherm temperatures were selected to be below T_p or the volatilization temperature that was determined using the TGA and rheology experiments.

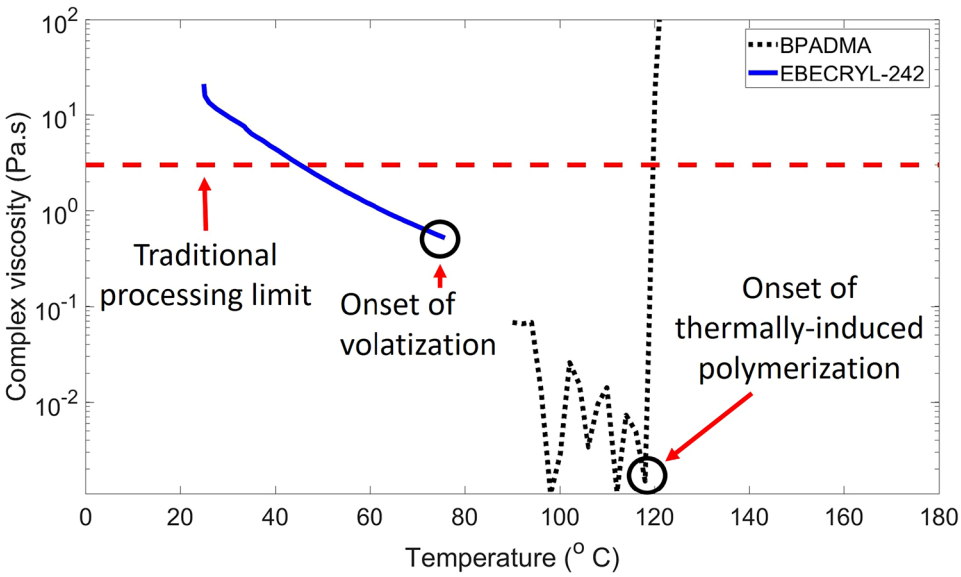

Fig. 3 Variable-temperature rheology of BPADMA indicates the occurrence of thermally induced polymerization at 118 °C. EBECRYL-242 resin undergoes volatilization before the onset of thermally induced polymerization

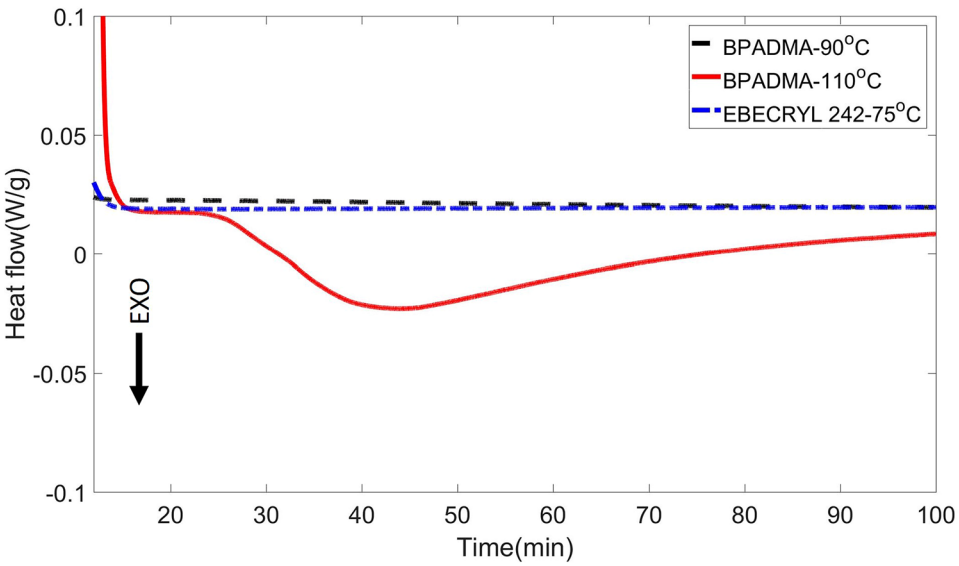

Fig. 4 The evolution of an exotherm within 30 min confirms thermally induced polymerization occurs in BPADMA when it is maintained at 110 °C whereas thermally induced polymerization is not observed in BPADMA maintained at 90 °C for 100 min. EBECRYL-242 resin does not undergo thermally induced polymerization when maintained at 75 °C for 100 min

From Fig. 4, it can be observed that the DSC of BPADMA at an isotherm of 90 °C does not contain an exothermic peak, indicating that thermally induced polymerization is not occurring in BPADMA for a duration of 100 min. However, an exothermic peak is observed at an isotherm of 110 °C, indicating the occurrence of thermally induced polymerization under 25 min of use (Fig. 4). Exploring isotherms in the range of 90–115 °C (SI-Figure SI 6) revealed (1) thermally induced polymerization occurred only beyond 110 °C, and (2) the onset of thermally induced polymerization occurred earlier when T_{print} exceed 110 °C (15 mins at 115 °C).

DSC of EBECRYL-242 at 75 °C does not show the presence of an exotherm, thus indicating that the resin does not undergo thermally induced polymerization for the entire duration of the experiment. DSC of EBECRYL-242 was not performed at temperatures exceeding 75 °C due to volatilization.

3.2 Interpretation of characterization results for process parameter selection

Understanding the dependence of thermal stability on printing time is critical for determining maximum printing time (t_{max}). If the time required to print a part exceeds t_{max}, then the resin will undergo thermally induced polymerization, leading to the build failure. However, given the variation in build volumes and printing technologies, specifying a universal printing temperature for a specific resin formulation is not feasible. Based on the exploration presented in this work, a general purpose framework is proposed for identifying the processing window for any combination of high-temperature VP technology and resin.

1. **Step 1**: Perform the resin characterization techniques listed in Sect. 2 and identify the degradation temperature (T_d), and the temperature at which onset of thermally induced polymerization is observed (T_p).
2. **Step 2**: For the printing technology in consideration, estimate the maximum printing time (t_{max}) for printing parts for the intended application. While estimating print time, consider factors such as build orientation, recoating time, exposure times for model and support layers.
3. **Step 3**: Perform isothermal DSC on the resin at temperatures slightly below T_p (or volatilization temperature) for a duration in the range of the estimated (t_{max}). Lower the isotherm temperature until no exotherm is observed to determine the printing temperature (T_{print}).
4. **Step 4**: Using the rheometer, determine the viscosity of the resin at the printing temperature (T_{print}). Evaluate if the resin viscosity at T_{print} is processable by the VP technology under consideration.
5. **Step 5**: Evaluate the resin curing parameters (i.e., depth of penetration and Critical Energy) by performing a cure depth study at T_{print}.
6. **Step 6**: Evaluate if the combination of the feature size, build orientation, green strength of cured network, and recoating technique are compatible for producing desired parts at T_{print} [10, 11]. Perform a screening DOE with factors such as printing temperature ($< T_{print}$), intensity, recoating speed, dosage to determine the printing parameter window for the characterized resin.
7. **Step 7**: Test the resin's usable life at elevated temperature by subjecting the resin to multiple heating and cooling cycles (T_{print} to $T_{ambient}$) using the isothermal DSC. The presence of an exothermal peak in the DSC trace will indicate the maximum cycles that the resin can be used

before onset of thermally induced polymerization. It must be noted that this approach neglects the depletion of photoinitiator in the resin with continuous use. Resin reconditioning may be required to maintain resin performance. The tools and techniques to recondition the resin are beyond the scope of this work.

8. **Step 8**: If resin is found to be producing undesirable results, reformulate the resin (alter photo-package, mixing ratio of resin components, or addition of crosslinkers) and repeat steps 1 through 7.

3.3 Verification of characterization results

Subjecting the two high-temperature resin systems to the resin characterization techniques outlined in Sect. 3.1 revealed that the T_d and T_p for EBECRYL-242 was approximately 75 °C and T_d and T_p for BPADMA was approximately 200 °C and 120 °C, respectively.

Using the printing parameters outlined in Table 2, the time required to fabricate the largest part in the custom high-temperature VP system was calculated to be (maximum dimensions: 20 × 30 × 30 mm) 60 min (t_{max}). Figure 4 and SI-Figure SI 6 show that BPADMA resin and EBECRYL-242 resins are least thermally stable for 100 min when processed at 100 and 75 °C, respectively, therefore, implying that the resins will not undergo thermally induced polymerization during part fabrication. Based on these results, T_{print} for BPADMA and EBECRYL-242 resins were selected to be 90 and 75 °C, respectively.

The viscosity of BPADMA and EBECRYL-242 resins at their T_{prints}, $\eta = 0.0683$ and 0.5188 Pa s, respectively, (Fig. 3), is less than the viscosity limit of the designed high-temperature VP apparatus ($\eta_{limit} < 10$ Pa s). Based on the geometry, feature size and orientation selected for the test artifacts, it was determined that the resin viscosity at the respective printing temperatures will not hinder part fabrication:

$$C_d = D_p \log\left(\frac{E}{E_c}\right), \text{ where } E = \left(\frac{N \times P}{h \times V_s}\right) \quad (1)$$

Using the working curve printing parameters outlined in Sect. 2.3.2, several test specimens were printed and measured. The exposure on the resin surface and the resin curing parameters (Critical energy (E_c) and Depth of penetration (D_p)) were determined using Eq. 1 [21]. Critical energy (E_c) and Depth of penetration (D_p) for EBECRYL-242 and BPADMA resins were determined using the working curves (EBECRYL: $E_c = 0.33$ mJ, $D_p = 310$ µm, BPADMA: $E_c = 0.05$ mJ, $D_p = 480$ µm, SI-Figure SI 5). Experimentally generated E_c and D_p were used to determine the exposure required for printing layers with a thickness of 120 µm. Layers printed with the determined exposure parameters exhibited sufficient green strength to support self-weight and handling, thus indicating parts with high-feature resolution could fabricated with these atypical photopolymer resins.

Specimens were successfully fabricated using the printing parameters (Laser Power (P), Scan speed (V_s), Hatch spacing (h) and No. of passes (N)) listed in Table 1 (Sect. 2.3.2).

Honeycomb printed with EBECRYL-242 resin (Fig. 5A) was flexible and did not deform plastically when compressed between the fingers. Tensile specimens fabricated with EBECRYL-242 resin exhibited elongations over 120 ± 6.5% with an average strength at break of 2.42 ± 0.31 MPa (SI-Figure SI 7). Since BPADMA produced highly crosslinked and brittle parts, it was used to print parts containing small features. The rook printed with BPADMA, (Fig. 5B, C) contained features in the size scale of 300 µm and they were printed successfully as shown in the inset of Fig. 5C.

Parts printed with BPADMA warped extensively when they were quenched in room temperature ethanol. This behavior is expected since BPADMA forms a highly crosslinked network that does not allow for polymer mobility and stress relief. Annealing BPADMA parts in olive oil maintained at 90 °C and slowly cooling to room temperature resulted in parts that were free from warping. It is hypothesized that the annealing process imparted mobility to the polymer chains allowing them to achieve a state with lowest amount of residual stresses.

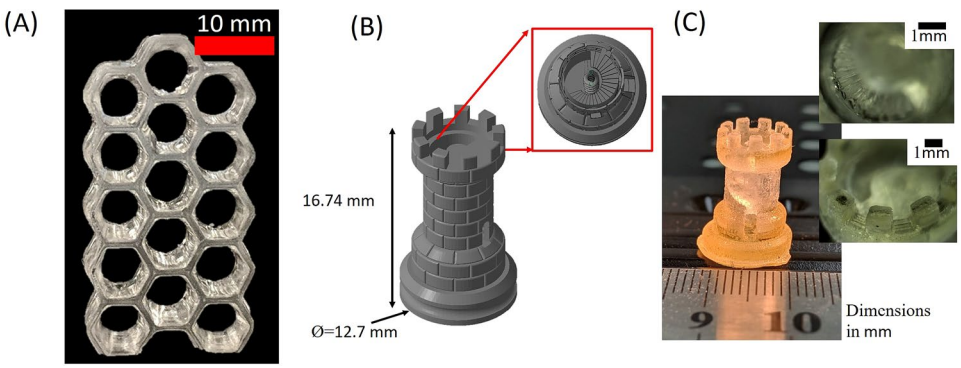

Fig. 5 **A** Honeycomb lattice printed with the EBECRYL-242 rein. **B**, **C** Rook printed with BPADMA exhibits fine features such as the staircase shown in the inset

Parts printed with EBECRYL-242 were immersed in ethanol (maintained at room temperature) for removal of cleaning and removal of uncured resin. Immersed parts did not exhibit signs of warping when they were quenched in ethanol immediately after printing at 75 °C. Since the printed parts remain under volatilization temperature, it is hypothesized that the EBECRYL-242 network remains plasticized by uncured IBOA and urethane acrylate oligomers, enabling it to reconfigure and relieve the thermal stresses, therefore preventing the warping of parts during quenching. Comparison of EBECRYL-242 parts quenched in hot olive oil and room temperature ethanol did not reveal visually identifiable difference in the Honeycomb structure.

Finally, self-initiated, cured fragments were not observed in the resins even after subjecting them to five thermal and printing cycles. While five cycles of reuse may not be sufficient to fully explore resin degradation at elevated temperatures, it provides confidence to the user that the developed resin characterization techniques are an appropriate means of identifying the printing temperature for safely processing photopolymers at elevated temperatures.

It must be noted that the post-process steps indicated in this work were developed for demonstration purposes only (i.e., that successful parts can be fabricated with characterization techniques presented in this work). While the development of appropriate post-processing methods, and reformulation strategies are highly formulation and application specific and is beyond the scope of this work, the following guidelines are proposed as a starting step for the users of high-viscosity resins and high-temperature VP systems:

1. Resin removal step: given the high viscosity of the resin, cleaning and removal of uncured resin from complex geometries may be more efficient when the part is hot. Users may consider the use of a hot cleaning medium (e.g., hot mineral oils) and physical agitation to remove residual resin from the parts.
2. UV post-curing step: UV post-curing may be used to foster the conversion of unreacted moieties in the green part and improve the mechanical properties of the printed parts.
3. Secondary thermal treatment step: additional heating and cooling cycles in an oven could be employed if warping or distortion is observed in the parts after UV post-curing.
4. Iteration step: Users may want to consider altering the printing parameters such as printing temperature, printing intensity, UV dosage or repeating the post-processing steps in different order to achieve desirable results.

3.4 Broader impacts of high-temperature vat photopolymerization and high-viscosity resins

In its current state, vat photopolymerization enables users to quickly prototype complex geometries with high resolution and surface finish. The use of simple acrylate, or methacrylate monomers blended with simple oligomeric backbones helps meet the requirements of the target audience. However, these simple photopolymer systems contain short chain monomers, and photoinitiators that are prone to extraction in aqueous media. These leachables pose a serious threat to human health and pose a challenge for safe disposal. While increased post-curing can help lower these risks by increasing the crosslinking in the polymer matrix, the variability in commercial photopolymers and lack of standardization in the post-process and material composition continue to elevate the risk of handling and disposing cured photopolymers [24]. It must be noted that the high-viscosity resins are not immune to the problems of excess leachables. While high molecular weight polymers used in viscous resins may be harder to extract in aqueous media, the viscous nature of the resin lowers polymer and radical mobility when processed with traditional VP systems. This often leads to the incomplete curing, low double bond conversion, and increased leachables in cured parts [15]. High-temperature vat photopolymerization systems not only allow for easy processing of viscous resins, but the method of processing the resins at elevated temperatures lends the following advantages:

1. Processing the resin at elevated temperatures lowers the resin viscosity, thus increasing the mobility of radicals and polymers. This increased mobility increases the likelihood of photopolymerization events, thus increasing the crosslink density, double bond conversion and simultaneously lowers the leachables
2. The combination of increased cross link density and low resin viscosity increases the green strength of the printed parts. This allows for printing of high resolution, high aspect ratio features which would have been previously inaccessible in traditional VP systems. This increase in design freedom allows for the use of structural optimization for generating engineered solutions for end use applications [5, 16, 19]
3. Processing photopolymers at elevated temperatures often alters the curing parameters, namely the critical energy(E_c) and the depth of penetration (D_p). Parts often need lower exposure time at elevated temperatures, thus leading to the formation of more pronounced layer lines in the part surface. This deterioration in surface finish may lower increase anisotropic behavior in the print direction. However, an overall improvement in geometric accuracy could be expected [19].

4. The removal of viscous resin from the printed parts often necessitates the use of heated post-processing procedures such as hot solvent/mineral oil wash (as described in Sec. 2.3.4) These post-processing of the parts at elevated temperatures provides more time for the polymer matrix to undergo rearrangement, thus allowing the fabrication of parts with minimal warping and internal stresses

While high-temperature vat photopolymerization offers several processing advantages, it must be noted that the selection of the polymer backbone, the final resin formulation, and the post-processing conditions have a strong influence on the performance and safety of the printed device. Given that the advancements in high temperature VP systems and performance photopolymers are fairly recent, the number of commercial machines and materials for high temperature VP are fairly limited and expensive. However, the growing interest to use polymer AM for manufacturing of mass customized products is expected to increase the research and development, and commercialization interests in the area of high-temperature vat photopolymerization.

4 Conclusion

The primary objective of this work was to develop a set of characterization techniques that helped determine the printing temperature that does not induce thermally initiated polymerization. To this end, two high-temperature VP resins, EBECRYL-242 and BPADMA, were formulated. First, TGA was used to determine the degradation and volatilization temperatures of the resins. Then, variable-temperature rheology was used to determine the temperature at which thermally induced polymerization occurred. Then, isothermal DSC was used to determine the time for which the resin remained thermally stable at different printing temperatures. A framework for interpreting and applying the characterization results for developing printing parameters was presented. The framework was applied to the EBECRYL-242 and BPADMA resins and the appropriate printing temperatures were determined to be 75 and 90 °C, respectively. The findings were validated using the predicted printing temperatures for successfully fabricating test specimens with BPADMA and EBECRYL-242 resins. In conclusion, the successful fabrication of specimens with previously inaccessible photopolymers provides evidence to support the use of the presented resin characterization techniques for determining the printing temperatures for high-temperature VP systems.

5 Supplementary information

Additional information about construction of the custom high-temperature VP system, working curves, and additional DSC isotherms can be found in the supplementary information.

Supplementary Information The online version contains supplementary material available at https://doi.org/10.1007/s40964-023-00562-0.

Acknowledgements The authors would like to thank Allnex for providing a free sample of EBECRYL-242 polymer.

The authors would like to thank the Materials Characterization Lab and Macromolecules Innovation Institute for providing access to the characterization instruments used in this work.

Funding This material is based upon work supported by the National Science Foundation under Grant No.: CMMI - 1762712.

Data availability Data available within the article or its supplementary materials. Additional data avaialable on request.

Declarations

Conflict of interest The authors have no relevant financial or non-financial interests to disclose.

References

1. Appuhamillage GA, Chartrain N, Meenakshisundaram V, Feller KD, Williams CB, Long TE (2019) 110th Anniversary: vat photopolymerization-based additive manufacturing: current trends and future directions in materials design. Ind Eng Chem Res 58(33):15109–15118. https://doi.org/10.1021/acs.iecr.9b02679
2. Tariq A, Arif ZU, Khalid MY, Hossain M, Rasool PI, Umer R, Ramakrishna S (2023) Recent advances in the additive manufacturing of stimuli-responsive soft polymers. Adv Eng Mater. https://doi.org/10.1002/adem.202301074
3. Ippolito R, Iuliano L, Gatto A (1995) Benchmarking of rapid prototyping techniques in terms of dimensional accuracy and surface finish. CIRP Ann Manuf Technol 44(1):157–160. https://doi.org/10.1016/S0007-8506(07)62296-3
4. Tumbleston JR, Shirvanyants D, Ermoshkin N, Janusziewicz R, Johnson AR, Kelly D, Chen K, Pinschmidt R, Rolland JP, Ermoshkin A, Samulski ET, DeSimone JM (2015) Continuous liquid interface production of 3D objects. Science 347(6228):1349–1352

5. Arif ZU, Khalid MY, Noroozi R, Sadeghianmaryan A, Jalalvand M, Hossain M (2022) Recent advances in 3D-printed polylactide and polycaprolactone-based biomaterials for tissue engineering applications. Int J Biol Macromol 218:930–968. https://doi.org/10.1016/j.ijbiomac.2022.07.140
6. Griffith M, Halloran J (1996) Freeform fabrication of ceramics via stereolithography. J Am Ceram Soc 79(10):2601–2608
7. Patel DK, Sakhaei AH, Layani M, Zhang B, Ge Q, Magdassi S (2017) Highly stretchable and UV curable elastomers for digital light processing based 3D printing. Adv Mater 29(15):1–7. https://doi.org/10.1002/adma.201606000
8. Hegde M, Meenakshisundaram V, Chartrain N, Sekhar S, Tafti D, Williams CB, Long TE (2017) 3D printing all-aromatic polyimides using mask-projection stereolithography: processing the nonprocessable. Adv Mater. https://doi.org/10.1002/adma.201701240
9. Herzberger J, Meenakshisundaram V, Williams CB, Long TE (2018) 3D printing all-aromatic polyimides using stereolithographic 3D printing of polyamic acid salts. ACS Macro Lett 7(4):493–497. https://doi.org/10.1021/acsmacrolett.8b00126
10. Li X, Mao H, Pan Y, Chen Y (2019) Mask video projection-based stereolithography with continuous resin flow. J Manuf Sci Eng Trans ASME 141(8):1–10. https://doi.org/10.1115/1.4043765
11. Renap K, Kruth JP (1995) Recoating issues in stereolithography. Rapid Prototyp J 1(3):4–16. https://doi.org/10.1108/13552549510094223
12. Song X, Chen Y, Lee TW, Wu S, Cheng L (2015) Ceramic fabrication using mask-image-projection-based stereolithography integrated with tape-casting. J Manuf Process 20:456–464. https://doi.org/10.1016/j.jmapro.2015.06.022
13. Hafkamp T, Baars G, Jager B, Etman P (2017) A trade-off/analysis of recoating methods for vat photopolymerization of ceramics. In: Solid freeform fabrication symposium, pp 1–25
14. Pan Y, Zhou C, Chen Y (2012) Rapid manufacturing in minutes: the development of a mask projection stereolithography process for high-speed fabrication. In: ASME 2012 international manufacturing science and engineering conference, p 405 . https://doi.org/10.1115/MSEC2012-7232. http://proceedings.asmedigitalcollection.asme.org/proceeding.aspx?doi=10.1115/MSEC2012-7232
15. Dickens SH, Stansbury JW, Choi KM, Floyd CJE (2003) Photopolymerization kinetics of methacrylate dental resins. Macromolecules 36(16):6043–6053. https://doi.org/10.1021/ma021675k
16. Schüller-Ravoo S, Zant E, Feijen J, Grijpma DW (2014) Preparation of a designed poly(trimethylene carbonate) microvascular network by stereolithography. Adv Healthc Mater 3(12):2004–2011. https://doi.org/10.1002/adhm.201400363
17. Gmeiner R (2018) Method and device for lithography-based generative production of three-dimensional moulds. https://patents.google.com/patent/EP3284583A1/en?oq=EP+3284583+A1
18. Li X, Xie B, Jin J, Chai Y, Chen Y (2018) 3D Printing temporary crown and bridge by temperature controlled mask image projection stereolithography. Procedia Manuf 26:1023–1033. https://doi.org/10.1016/j.promfg.2018.07.134
19. Steyrer B, Busetti B, Harakály G, Liska R, Stampfl J (2018) Hot lithography vs. room temperature DLP 3D-printing of a dimethacrylate. Addit Manuf 21(January):209–214. https://doi.org/10.1016/j.addma.2018.03.013
20. Riazi H, Shamsabadi A, Grady MC, Rappe AM, Soroush M (2018) Experimental and theoretical study of the self-initiation reaction of methyl acrylate in free-radical polymerization. Ind Eng Chem Res 57(2):532–539. https://doi.org/10.1021/acs.iecr.7b04648
21. Jacobs PF (1992) Rapid prototyping and manufacturing. Fundamentals of stereolithography, 1st edn. Society of Manufacturing Engineers (1992)
22. Ors JA, La Perriere DM (1986) Thermogravimetric profile of decomposition of acrylate systems based on bornyl acrylate monomers. Polymer 27(12):1999–2002. https://doi.org/10.1016/0032-3861(86)90197-7
23. Pham QT, Hsu JM, Pan JP, Wang TH, Chern CS (2013) Kinetics of free radical polymerization of bisphenol A diglycidyl ether diacrylate initiated by barbituric acid. Thermochim Acta 573:121–129. https://doi.org/10.1016/j.tca.2013.09.002
24. Carve M, Wlodkowic D (2018) 3D-printed chips: compatibility of additive manufacturing photopolymeric substrata with biological applications. Micromachines 9(2):91. https://doi.org/10.3390/mi9020091

Terms and Conditions

Springer Nature journal content, brought to you courtesy of Springer Nature Customer Service Center GmbH (“Springer Nature”).
Springer Nature supports a reasonable amount of sharing of research papers by authors, subscribers and authorised users (“Users”), for small-scale personal, non-commercial use provided that all copyright, trade and service marks and other proprietary notices are maintained. By accessing, sharing, receiving or otherwise using the Springer Nature journal content you agree to these terms of use (“Terms”). For these purposes, Springer Nature considers academic use (by researchers and students) to be non-commercial.
These Terms are supplementary and will apply in addition to any applicable website terms and conditions, a relevant site licence or a personal subscription. These Terms will prevail over any conflict or ambiguity with regards to the relevant terms, a site licence or a personal subscription (to the extent of the conflict or ambiguity only). For Creative Commons-licensed articles, the terms of the Creative Commons license used will apply.
We collect and use personal data to provide access to the Springer Nature journal content. We may also use these personal data internally within ResearchGate and Springer Nature and as agreed share it, in an anonymised way, for purposes of tracking, analysis and reporting. We will not otherwise disclose your personal data outside the ResearchGate or the Springer Nature group of companies unless we have your permission as detailed in the Privacy Policy.
While Users may use the Springer Nature journal content for small scale, personal non-commercial use, it is important to note that Users may not:

1. use such content for the purpose of providing other users with access on a regular or large scale basis or as a means to circumvent access control;
2. use such content where to do so would be considered a criminal or statutory offence in any jurisdiction, or gives rise to civil liability, or is otherwise unlawful;
3. falsely or misleadingly imply or suggest endorsement, approval , sponsorship, or association unless explicitly agreed to by Springer Nature in writing;
4. use bots or other automated methods to access the content or redirect messages
5. override any security feature or exclusionary protocol; or
6. share the content in order to create substitute for Springer Nature products or services or a systematic database of Springer Nature journal content.

In line with the restriction against commercial use, Springer Nature does not permit the creation of a product or service that creates revenue, royalties, rent or income from our content or its inclusion as part of a paid for service or for other commercial gain. Springer Nature journal content cannot be used for inter-library loans and librarians may not upload Springer Nature journal content on a large scale into their, or any other, institutional repository.
These terms of use are reviewed regularly and may be amended at any time. Springer Nature is not obligated to publish any information or content on this website and may remove it or features or functionality at our sole discretion, at any time with or without notice. Springer Nature may revoke this licence to you at any time and remove access to any copies of the Springer Nature journal content which have been saved.
To the fullest extent permitted by law, Springer Nature makes no warranties, representations or guarantees to Users, either express or implied with respect to the Springer nature journal content and all parties disclaim and waive any implied warranties or warranties imposed by law, including merchantability or fitness for any particular purpose.
Please note that these rights do not automatically extend to content, data or other material published by Springer Nature that may be licensed from third parties.
If you would like to use or distribute our Springer Nature journal content to a wider audience or on a regular basis or in any other manner not expressly permitted by these Terms, please contact Springer Nature at

onlineservice@springernature.com